

Microsimulation analysis of practical aspects of traffic control with variable speed limits

Eduardo R. Müller, Rodrigo C. Carlson, *Member, IEEE*
 Werner Kraus Jr., *Member, IEEE*, and Markos Papageorgiou, *Fellow, IEEE*

Abstract—Mainstream Traffic Flow Control (MTFC) with Variable Speed Limits (VSL) is a freeway traffic control method which aims to maximize throughput by regulating the mainstream flow upstream from a bottleneck. Previous studies in a macroscopic simulator have shown optimal and feedback MTFC potential to improve traffic conditions. In this paper, local feedback MTFC is applied in microscopic simulation for an on-ramp merge bottleneck. Traffic behavior reveals important aspects that had not been previously captured in macroscopic simulation. Mainly, the more realistic VSL application at specific points instead of along an entire freeway section produces a slower traffic response to speed limit changes. In addition, the nonlinear capacity flow/speed limit relation observed in the microscopic model is more pronounced than what was observed at the macroscopic level. After appropriate modifications in the control law significant improvements in traffic conditions are obtained.

Index Terms—Mainstream traffic flow control. Freeway traffic control. Variable speed limits. Microscopic traffic simulation.

I. INTRODUCTION

TRAFFIC congestion is a main problem in metropolitan areas. Congestion is known to reduce the capacity of freeways [1], with consequences such as increased vehicular delays, reduced traffic safety, driver stress, and environmental pollution. Traffic control is seen as a way to prevent or at least delay the onset of congestion hence improving traffic conditions.

In the past decade, Variable Speed Limits (VSL) have emerged as a potential traffic management tool for increasing freeway efficiency, in contrast to earlier safety-oriented applications. Since then, some works focused on studying the effects of VSL on traffic behavior, e.g., [2]–[4], while others proposed traffic management strategies based on different design methodologies and system configurations, such as shockwave theory [5], feedback control [6], optimal control [7], and model predictive control [8], just to cite a few. Despite

The first and third authors were funded by CNPq, Brazil. For the research leading to these results, the last co-author has received funding from the European Research Council under the European Union's Seventh Framework Programme (FP/2007-2013)/ERC Advanced Investigator Grant Agreement no. 321132, project TRAMAN21.

E. R. Müller and W. Kraus Jr. are with the Post-graduate Program in Automation and Systems Engineering, Federal University of Santa Catarina, Florianópolis-SC, 88040-900 Brazil edurauh@gmail.com; werner.kraus@ufsc.br

R. C. Carlson is with the Post-graduate Program in Automation and Systems Engineering, and with the Center for Mobility Engineering, Federal University of Santa Catarina, Joinville-SC, 89218-000 Brazil rodrigo.carlson@ufsc.br

M. Papageorgiou is with the Department of Production Engineering and Management, Technical University of Crete, Chania, 73132 Greece markos@dssl.tuc.gr

of these advances, field implementations of such strategies have not been reported, with the exception of the successful field trial of the SPECIALIST strategy [9].

Mainstream Traffic Flow Control (MTFC) on freeways by use of VSL [10]–[13] aims to maximize throughput by regulating the mainstream flow upstream from a bottleneck and has shown promising results in simulation. Studies evaluated both an optimal control approach with exact prediction of traffic flows [11] and a more realistic feedback scheme deemed suitable for field applications [12]. These studies were carried using a second-order macroscopic simulation environment, namely the METANET simulator [14], which does not model some details that could be interesting from a practical perspective. Therefore, those results are refined here with a microscopic traffic simulator, since with the METANET model:

- speed limit changes affect a whole freeway section, while in reality the change usually affects vehicles that are passing by the point where the speed limit is posted;
- as used in previous studies, traffic is deterministic, whereas real traffic systems are stochastic;
- space and time are discretized in the form of segments with a given length and simulation time step, which may restrict admissible lengths for control application.

Although studies [15], [16] question the ability of current microscopic lane-change models to accurately capture merging behavior in a congested regime, we consider that:

- appropriate application of MTFC can prevent the onset of congestion at the bottleneck, therefore establishing a regime where lane-change models are more accurate;
- a controlled congestion in the application area far upstream from the bottleneck will not be affected by lane-changing behavior at the merge area;
- despite the microscopic merging behavior, the model was adjusted to give a capacity drop in the aggregate traffic behavior similar to practical values [17].

In this paper we use the Aimsun Microscopic Traffic Simulator [18]. Aimsun implements two vehicle behavior models: car-following and lane-changing, both of which can be considered as developments of the respective Gipps models [19], [20]. The Aimsun implementation allows a non-deterministic range of values to be set for several vehicle parameters (i.e., each vehicle can have its own acceleration, deceleration, etc., randomly sampled from customizable probability distributions).

Applying feedback MTFC-VSL to a freeway stretch in Aimsun reveals important aspects of the control method that

were not considered in previous studies. This paper presents the following findings:

- for the studied scenario, the relation between flow and speed limits shows a stronger nonlinearity than what was observed in previous studies, see, e.g., [13];
- when speed limit changes do not affect a whole section, i.e., affect only vehicles passing by the posted speed limit, a slower traffic response results, especially for increasing speed limits;
- the length of the section where VSL is applied and the distance between this section and the bottleneck to be controlled affect the speed of the traffic response to VSL changes;
- overall, microscopic simulations confirm that MTFC-VSL can successfully avoid the capacity drop and the onset of congestion, thereby increasing the performance of a freeway bottleneck.

Previous works about VSL control strategies in microscopic simulation environments [6], [21]–[23] focused mainly on system performance whereas the present study focuses also on features that affect control design and, as such, anticipates practical aspects that may appear in reality. A brief review of mainstream traffic flow control can be found in [12]. Reviews of the use of VSL for freeway traffic control can be found in [24], [25]. The feedback MTFC scheme in [12] was extended in [26] to consider the presence of multiple bottlenecks.

The next section briefly presents the MTFC concept, the controller design and elaborates on practical control aspects. Section III presents the simulations goals and setup, as well as the controller setup. Section IV presents simulation results. Conclusions are presented in Section V.

II. MTFC-VSL AND CONTROLLER DESIGN

A. The MTFC Concept

MTFC is a freeway traffic control method which aims to maximize freeway throughput by controlling the mainstream traffic flow. The idea is to keep the mainstream traffic flow upstream from a bottleneck at a sufficiently low level to avoid congestion and capacity drop at the bottleneck location, establishing maximum flow.

It is inevitable that by doing so, MTFC induces a controlled congestion at the location where MTFC is applied. This congestion, however, is located upstream of the bottleneck. Thus, it avoids the capacity drop and produces higher outflow and speed than in the no-control case. In this work we consider VSL as an MTFC actuator, based on the principle that lower speed limits induce lower capacity flows [10].

We denote the area subject to VSL as the *application area*. Vehicles may leave this area with low speeds, so for them to reach the critical speed v_{cr} (corresponding to the bottleneck capacity flow at the critical occupancy o_{cr}) at the bottleneck, the end of the area should be sufficiently upstream of the bottleneck. The section between the application area and the bottleneck is denoted the *acceleration area*. Figure 1 depicts both areas for an on-ramp bottleneck.

B. Feedback MTFC-VSL

The control problem is to regulate the occupancy o_{out} of the bottleneck at a reference value (set-point) \hat{o}_{out} by controlling with VSL the mainstream flow upstream of the bottleneck. We define a VSL rate $0 < b \leq 1$ as the ratio of the current speed limit by the nominal speed limit. This is a single-input-single-output control problem where the VSL rate b and occupancy o_{out} are the control action and controlled variable, respectively. A discrete-time linear model for this system is given by [12]:

$$\frac{\Delta o_{out}(z)}{\Delta b(z)} = K' \cdot \frac{\tau}{z + \tau - 1} \cdot K \frac{z - \alpha}{z - \beta} \quad (1)$$

with $\alpha, \beta, \tau > 0$, and $K > 0$ being model parameters, and $0 < \beta < \alpha \leq 1$; z is the discrete-time complex variable; Δo_{out} is the occupancy variation caused by VSL rate variation Δb . The model (1) is a transfer function describing the input-output relation of the traffic behaviour of the freeway. On the right hand side, the last term describes the dynamic behaviour of q_c due to a speed limit variation (via VSL rate b), the middle term describes the smoothed and delayed propagation of flow through the acceleration area, and the left term the static translation of the inflow to the bottleneck into bottleneck occupancy. A detailed account of the modelling process is provided in [12].

Based on model (1) an I-type control structure can be used to calculate the VSL rate b at instant k :

$$b(k) = b(k-1) + K_I e_o(k) \quad (2)$$

with K_I the integral gain of the controller and $e_o(k) = \hat{o}_{out} - o_{out}(k)$ the occupancy control error, with occupancy in %. We set \hat{o}_{out} equal to the critical occupancy o_{cr} for maximum flow. This control structure was chosen mainly because of its simplicity (which makes it easier to tune) and showed good performance in the simulated scenarios. The interested reader may verify the design of (2) based on (1) by the use of standard control systems analysis and design tools, see, e.g., [27].

It should be noted that in [13] a cascade and a PI control structure were applied, possibly because of the long acceleration areas used. In [28] an I-controller was used to relocate congestion away from populated areas; performance was also a concern but capacity drop did appear even under control.

C. Nonlinearity of the Capacity Flow/Speed Limit Relation

The shape of the capacity flow/speed limit relation for the range of allowed speed limits reflects the linearity of the system and, thus, serves as an indication of the suitability of the linear control law (2). Figure 2 depicts three normalized capacity flow/speed limit curves, including one obtained by [13] with the METANET macroscopic simulator [14] (solid

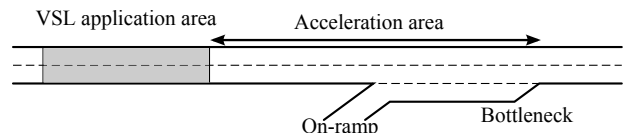


Fig. 1. MTFC-VSL application and acceleration areas

line) and one obtained in this work with the Aimsun microscopic simulator (dashed line). For each curve, normalization is performed by dividing the flow observed with each speed limit by the highest flow observed (i.e., with a nominal speed limit of 100 km/h). See [13] for details on how to obtain this curve.

By inspection of Fig. 2, one can see that the Aimsun curve looks more nonlinear than METANET's. We use the least squares method [29] to compare these two curves in a quantitative way. We compute the quadratic error of each curve in relation to the line segment that best fits it through the least squares method, and use this value as an indicator of how linear each curve is. The lower the error obtained, the more the curve approaches a linear relation. After normalizing the two curves in Fig. 2 in the abscissa axis (dividing all speed limits by 100) and performing the aforementioned procedure, the values of 0.053 and 0.020 were obtained for the Aimsun and METANET curves, respectively. Thus, the capacity flow/speed limit relation obtained with Aimsun is more nonlinear than that obtained with METANET.

In [13] the METANET capacity flow/speed limit relation shown in Fig. 2 is approximated as linear with good results. However, the more pronounced nonlinearity obtained with Aimsun suggests that a different approach should be sought since traffic response at very different speed regimes (e.g., 80 km/h and 20 km/h) is significantly different, rendering the system difficult to be controlled with a linear controller.

It is hard to know which curve is closer to reality, since there are few studies about the effects of speed limits in freeway capacity. See, e.g., [2] and references therein. We can, however, compare the curves with a simplified model.

In order to perform a simplified analysis on the effects of variable speed limits in the traffic state, consider two hypotheses:

- Consider a flow-density fundamental diagram with a triangular shape as the one in Fig. 3.
- Consider that the speed at which a vehicle travels is the lowest between the speed resulting from the traffic conditions and the posted speed limit. That is, the traffic state is bounded to be below both the original fundamental diagram and the line segment with slope given by the speed limit. Such consideration is like the one proposed

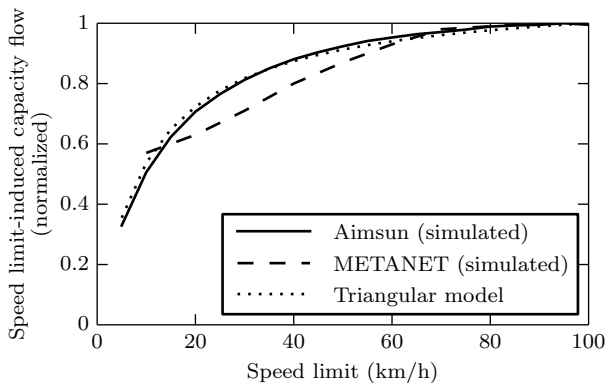


Fig. 2. Normalized capacity flow/speed limit relation

in [30]. In this way, the application of a speed limit v_2 affects the shape of the left side of the fundamental diagram (Fig. 3), forcing the admissible traffic states to be “below” the line segment with slope v_2 that goes through the origin. A traffic state that is above this line segment would need to have, by definition, a higher speed than the speed limit. Thus, lower speed limits affect the fundamental diagram inducing lower capacity and higher critical occupancy.

Now, consider two distinct traffic states, represented by two points (A and B) in the fundamental diagram, as illustrated in Fig. 3:

- Point A is the critical point (for the nominal speed limit), in which the freeway is operating at maximum capacity q_{cap} . By definition, this point has critical density ρ_{cr} and critical speed v_{cr} .
- Point B when subject to a lower speed limit, v_2 , is also critical. Speed limit v_2 induces a capacity q_2 , obtained in the point where the line segment with slope v_2 that goes through the origin meets the nominal fundamental diagram. Density in this state is given by ρ_2 .

Given these considerations, by analysing Fig. 3, we can geometrically derive the freeway capacity $q_{cap}(v_2) = q_2$ induced by a speed limit v_2 as

$$q_2 = \frac{w + v_{cr}}{w + v_2} \cdot \rho_{cr} \cdot v_2, \quad (3)$$

where ρ_{cr} , v_{cr} and w are parameters that can be obtained empirically. This relation is nonlinear, and q_2 is more sensitive to v_2 at lower speed limits.

To compare results given by this model with the relation obtained through simulation with Aimsun, we can derive the value of these parameters based on simulator parameters and simulation results for the no control case (Section IV): $q_{cap} = 1850$ veh/h/lane, $\rho_{cr} = 19\%$, with corresponding $\rho_{cr} = 25$ veh/km/lane, $v_{cr} = 85$ km/h, and $w = 10.57$ km/h. Based on (3), a capacity flow/speed limit curve corresponding to these parameters can be drawn. The dotted curve in Fig. 2, labeled “triangular model”, corresponds to this relation.

It is clear that the curve obtained with this simplified model is very close to the curve obtained through simulation

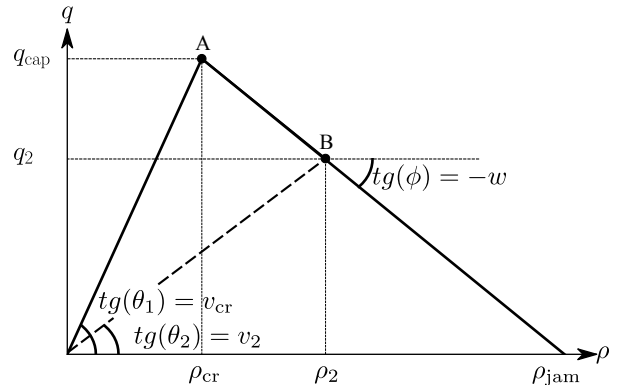


Fig. 3. Flow-density triangular fundamental diagram. Effect of a speed limit v_2

with Aimsun. The fact that the simplified model used in this analysis correlates more to the results obtained with Aimsun does not necessarily mean this model is closer to reality than the METANET model. Regardless, it is important to note that the capacity flow/speed limit relation obtained with both simulators are significantly different, and that they have an impact in system dynamics and controller performance. Should MTFC-VSL be applied in a real location, the study and validation of this relation is an important step before implementation.

D. Feedback MTFC-VSL with Gain Scheduling

The nonlinear capacity flow/speed limit relation discussed in the previous section makes a linear control strategy such as (2) inadequate to maintain stability at all allowed speed limits, unless a slow control reaction at high speed limits is tolerated. To circumvent this problem, gain scheduling [31] is adopted.

With gain scheduling, different integral gains are assigned for different operation points. The VSL rate b is used to determine the current point of operation and then the appropriate gain is selected. The definition of appropriate gains is discussed in Section III.

E. Structural Control Aspects

The implementation of MTFC-VSL requires the definition of the way speed limits are imposed, and of the lengths of the application and acceleration areas. These aspects affect system dynamics and are discussed in this section.

1) *Ways of applying VSL*: we examine two possible ways of applying VSL. In Section Level VSL (S-VSL), VSL is applied to a whole freeway section; i.e., all vehicles within the application area immediately adjust their speeds to the new speed limit. At the macroscopic level, only S-VSL is possible. In reality S-VSL requires vehicle-infrastructure integration systems, such as in [32], or tightly spaced VSL signs.

In contrast, Point Level VSL (P-VSL) considers a more typical sparse distribution of VSL signs, whereby vehicles adjust their speed when passing by the VSL sign and maintain this speed until a new sign indicates a different speed limit further downstream. Hence, with P-VSL a change in the speed limit affects only vehicles arriving at the application area with no effect on vehicles already inside it.

Testing in Aimsun revealed that with P-VSL:

- as could be expected, traffic response to speed limit changes is slower than with S-VSL, i.e., it takes longer for changes to have an effect on the merging area;
- the effects on traffic of a VSL increase take longer to appear than when VSL is decreased; it should be noted that in the modeling of [33], a similar behavior can be observed but the authors did not elaborate on its cause;
- a temporary ‘void’ of vehicles may be formed in the mainstream ahead of the application point when VSL is decreased.

The space-time diagrams in Fig. 4 illustrate these findings for an hypothetical freeway section with an application area from d_1 to d_2 . In a microscopic simulation, VSL changes

between v and v' , with $v > v'$. The speed limit upstream and downstream of the application area is v .

For the P-VSL case (Fig. 4(a–b)), a VSL sign is placed at the entrance of the application area. Fig. 4(a) depicts a VSL increase from v' to v at time t_1 . Vehicles entering the VSL application area are unable to maintain speed v because of the presence of slower vehicles ahead moving at speed v' (dark area). The delay between increasing the VSL and observing vehicles at the desired speed leaving the application area varies according to the difference between v and v' and the length of the application area.

Fig. 4(b) depicts a VSL decrease from v to v' at time t_1 . Vehicles in the application area at the time of the speed limit change maintain speed v , while new ones enter the application area with speed v' . Thus, the distance between the rear of the faster platoon and the front of the slower one increases over time, leading to a temporary ‘void’ of vehicles. If the application area is sufficiently long and the new speed limit v' is sufficiently smaller than v , this leads to a temporary and significant decrease in flow (and occupancy) downstream until vehicles traveling at speed v' reach the bottleneck. If the speed limit v' is sufficiently low and the demand sufficiently high, the outflow after the void has passed will be lower than under speed limit v .

Fig. 4(c–d) depict the corresponding cases for S-VSL. Clearly, traffic response is faster in these cases and, consequently, easier to control. Although currently not feasible from a practical standpoint, the use of S-VSL in field applications would give the best performance.

2) *Length of the application area*: the discussion about P-VSL and S-VSL in the previous section indicates that if P-VSL is used, longer VSL application areas lead to longer delays and a slower system, which is undesirable. The effect of the length of the application area on the traffic response and system performance is investigated in Section IV.

3) *Length of the acceleration area*: longer acceleration areas lead to higher delays in both forms of VSL application, since vehicles leaving the VSL application area have to cover a longer distance to reach the bottleneck. This effect should be less pronounced than the delay caused by larger application areas, since vehicles usually travel considerably faster in the acceleration area than in the application area.

More importantly, the length of the acceleration area also has an effect on the speed at which vehicles reach the bottleneck (e.g., an acceleration area that is too short might be insufficient for vehicles to accelerate to v_{cr}). Reaching the bottleneck with an inadequate speed may compromise vehicle merging behavior, decreasing system performance. It follows that there should be an optimal length or range of lengths for the acceleration area. The effect of the length of the acceleration area on the traffic response and system performance is investigated in Section IV.

F. Field Deployment Aspects

There are certain practical aspects that should be considered before a field deployment of VSL. They are mainly the discretization of speed limits and the limiting of space and

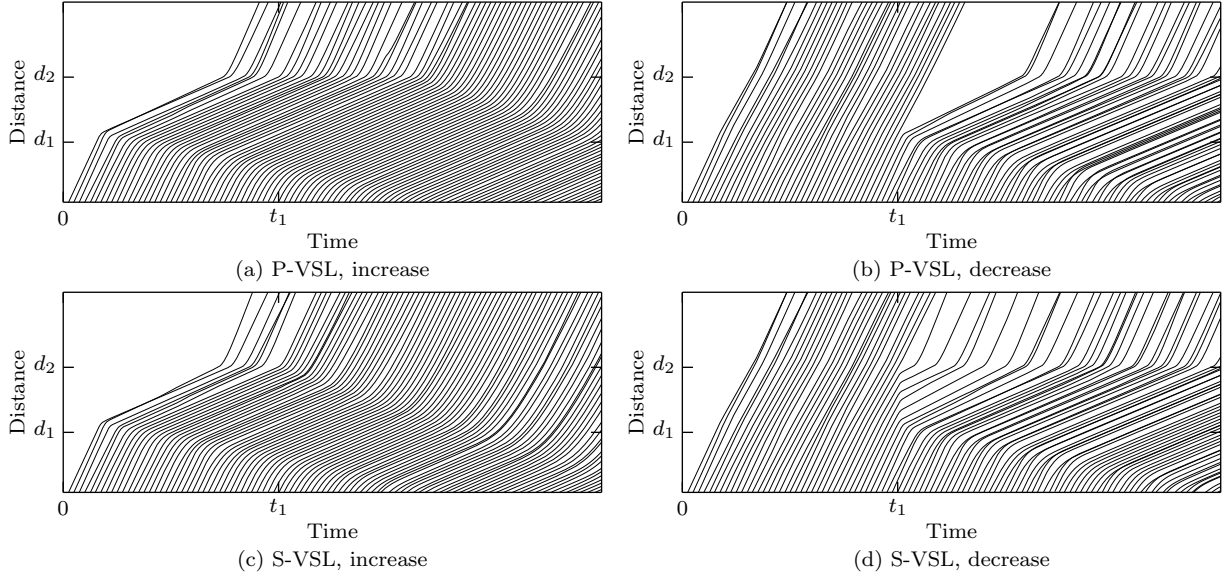


Fig. 4. Space-time diagrams for point (P) and section (S) VSL application

time for VSL variation. Although already considered in other works, such as [12], it is interesting to assess the effect of these aspects in microscopic simulation.

1) *Discrete VSL*: the control algorithm delivers real values for the VSL. However, such values may be unsuitable for practical application. If that is the case, the speed limit should be rounded to a value contained in a predefined set of allowed speed limits, such as $VSL \in \{10, 20, \dots, 90, 100\}$ km/h.

2) *Limited VSL time and space variation*: it may be argued that (for safety concerns) drivers should not be subject to large and sudden speed limit changes, both in space and time. To address time variation, the difference between two consecutive speed limits posted at the same sign can be limited to not exceed a determined value, e.g., 20 km/h at time steps not less than, say, 1 min. To address space variation, it is necessary to have multiple adjacent application areas, where each one imposes a speed limit which is at most 20 km/h higher than the one immediately downstream (or the nominal speed limit, whichever is lower). The most downstream area simply imposes the speed limit corresponding to the VSL value computed by the control algorithm. Depending of the range of allowed speed limits, a different number of application areas may be necessary.

3) *Driver compliance to the displayed VSL*: driver compliance is an important aspect for VSL systems, and, in extreme cases of very low compliance, any VSL-based system may indeed be factually invalidated. But a varying driver compliance within reasonable levels has only a minor impact on the feedback dynamics, and hence it is not explicitly considered in this work. Typically, low compliance implies an average speed slightly higher than the posted speed limit, and therefore a higher outflow than the one that is desired for a given speed limit. With feedback control, a lower speed limit will be ordered until the flow is sufficiently low or the lower bound is reached. For related details, the reader is referred to [12].

III. SIMULATION SETUP

This section discusses the goals of the simulations performed and presents the modeled network and demands used.

A. Simulation Goals

Our purpose is to study how different setups affect MTFC-VSL. A simple hypothetical network is used with a demand sufficiently high to ensure congestion occurs in the no-control case. Different scenarios are simulated in order to test the influence of the following aspects in system performance: gain scheduling; way of applying VSL (P-VSL versus S-VSL); length of VSL application and acceleration areas; VSL discretization (quantization); and limited variations in time and space for VSL indications.

B. Network Model and Demand

Figure 5 shows the simulated 4.3 km hypothetical freeway stretch with two lanes and one on-ramp 300 m upstream of its end. A 200 m acceleration lane creates the merge area with a lane drop where the bottleneck is formed. The nominal speed limit is 100 km/h.

The demand profiles in Fig. 6 extending over a 3-hour simulation period are used as traffic inputs. A normal distribution with standard deviation of 10% from the mean is used to sample entrance times.

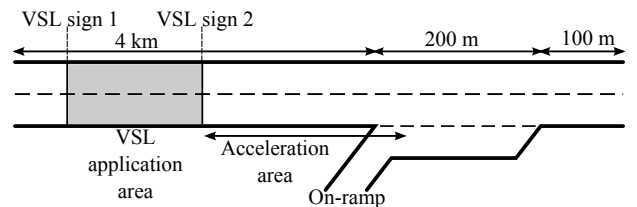


Fig. 5. Hypothetical network (not in scale)

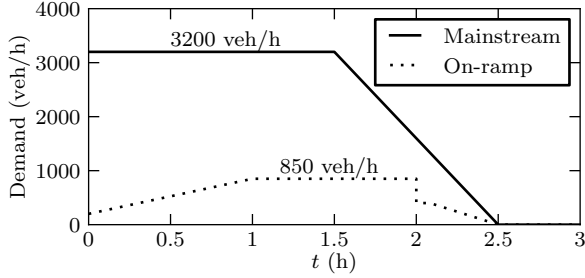


Fig. 6. Simulated demand

C. Simulator Parameters

Traffic is comprised of passenger cars. Default values of the simulator were used for most parameters, except for reaction time (0.5 s), vehicle acceleration (1.5 m/s^2) and parameters for the two-lane car following model, which were adjusted for a maximum speed difference of 30 km/h between mainstream lanes and 50 km/h between the rightmost and middle lanes in the three-lane section. These values give a nominal capacity of 3700 veh/h and a capacity drop of around 17% for the studied demands, in line with field observations [17].

D. Controller Parameters

1) *Integral gain*: the controller is first tuned for a fixed integral gain to be used with the linear control law (2). Empirical tuning for the best performance indicates the value of $K_I = 0.005$. Then, a set of integral gains is selected for different ranges of VSL rate b for the use with gain scheduling. Figure 7 shows the capacity flow/speed limit relation obtained through simulation. Using piecewise linear regression we obtained the minimum quadratic error with the three line segments shown in the figure.

For a nominal speed limit of 100 km/h, the resulting ranges for the three segments and respective gains are approximately: $0 < b \leq 0.3$ and $K_I = 0.004$; $0.3 < b \leq 0.5$ and $K_I = 0.012$; and $0.5 < b \leq 1$ and $K_I = 0.045$. The gains are proportional to the ratios between the slopes of the respective line segments. With these, the control strategy is fast at high speed limits and remains stable at low ones, providing sufficiently good performance.

Note that these values and Fig. 7 are different from those previously used in [34]. The difference is due to the fact

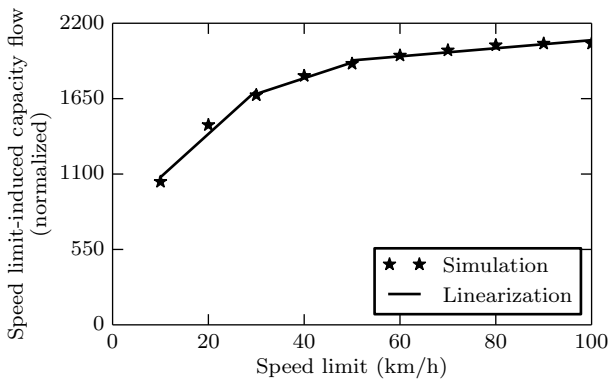


Fig. 7. Piecewise linearization of the capacity flow/speed limit relation

that less points of the capacity flow/speed limit curve are considered when performing the piecewise linearization in the present work, so different line segments are obtained. This change is made because the previous piecewise linearization resulted in specific gains for very narrow ranges of b , and the lowest gain was actually rarely used. By considering less points broader ranges of b for the two lower gains are obtained, so the gain decreases sooner. Because of this, simulation results for most scenarios are also different in this paper.

2) *Set-point*: a critical occupancy o_{cr} of 19% is found from the no-control scenario (see Section IV). This value is used as the set-point \hat{o}_{out} in all control scenarios. The critical speed is around 85 km/h.

E. Occupancy measurement

In the simulated scenario, the merge point of on-ramp and mainstream vehicles changes according to the incoming flows. When traffic is low, vehicles are able to change lanes more easily and thus merging happens closer to the on-ramp. Near breakdown, merging is usually closer to the lane drop. Since each detector has a limited coverage area more than one detector is needed for a proper occupancy measurement, as sometimes congestion may start forming far downstream or upstream from a given detector.

For this reason, five detectors are placed spaced 50 m apart in the 200 m area between the on-ramp and the lane drop. The highest measured occupancy at each interval is taken as the control measurement. In the majority of control intervals, this corresponds to the readings taken in the middle detector.

IV. SIMULATION RESULTS

Simulation results correspond to the mean of 10 replications using different random seeds. Table I summarizes the results for the tested scenarios. Its columns correspond to the scenario number, whether gain scheduling is being used, the length of the application and acceleration areas, the way of applying VSL, the Total Time Spent (TTS), and the TTS reduction in relation to the no control case. For scenarios 7 to 9, various discretization possibilities are considered.

Flows, occupancies, speeds, and VSL rates are shown in Figs. 8 and 10, always corresponding to the replication that showed the TTS closest to the mean. Dotted lines denote the set-point. The graphics presented show flow measurements corresponding to the total of all three lanes, while occupancy and speeds correspond to the mean of the two mainstream lanes.

It is important to note that the purpose of the present work is not to verify how much MTFC-VSL can improve traffic, but to study how different control setups affect MTFC-VSL. Therefore, improvement in relation to the no-control scenario should be viewed mainly as a measure for comparing two different control scenarios and not as an absolute measure of performance.

A. Base Scenarios

Table I, rows 1–3, summarizes the base scenarios with flows, occupancies, speeds, and VSL rates shown in Fig. 8(a–c).

TABLE I
SUMMARY OF SIMULATED SCENARIOS

Scn.	Gain Sched.	App/Acc. areas lengths (m)	VSL type	TTS (veh-h)	%
1	–	–	–	1137	–
2	No	300/275	P-VSL	787	–30.8
3	Yes	300/275	P-VSL	676	–40.6
4	Yes	300/275	S-VSL	621	–45.4
5	Yes	100/275	P-VSL	606	–46.7
6	Yes	300/175	P-VSL	646	–43.2
				TTS (veh-h)	%
7	Scn. 3 + Discrete VSL			803	–29.4
8	Scn. 7 + Limited VSL time variation			842	–25.9
9	Scn. 8 + Limited VSL space variation			989	–13.0

Application and acceleration areas are fixed and P-VSL is used for MTFC-VSL.

1) *Scenario 1 - No control (Fig. 8(a))*: the congestion formed at $t = 0.7$ h leads gradually from a capacity flow of 3700 veh/h to an outflow of 3070 veh/h, a drop of 17%. Despite the decreasing demand entering the network after $t = 1.5$ h, it takes until $t = 2.5$ h before congestion is dissolved. The Total Time Spent by all vehicles during simulation is equal to 1137 veh-h.

2) *Scenario 2 - Integral control with fixed gain (Fig. 8(b))*: the slow reaction of the controller causes a peak in occupancy at around $t = 0.8$ h. The peak is followed by large variations in flow and occupancy (and in the control action b) around the set-point, which is undesirable despite the decrease in TTS of 30.8%. A gain increase aiming for a faster reaction of the controller would turn the system oscillatory or even unstable at low speed limits.

3) *Scenario 3 - Integral control with gain scheduling (Fig. 8(c))*: the controller reacts faster at high speed limits with smoother action at low speed limits when compared to the previous scenario. Capacity flow and critical occupancy are maintained most of the time with an improvement in TTS of 40.6%. The flow dip at $t = 1.0$ h reflects the control reaction to a sudden increase in occupancy. The value of K_I for b between 1.0 and 0.5 is considerably larger than the fixed gain used in Scenario 2, allowing the earlier reaction seen for t between 0.5 and 1 h. All the following scenarios also consider the use of gain scheduling.

B. Point versus Section VSL Application

Scenario 4 in Table I is analogous to Scenario 3 but with S-VSL instead of P-VSL. Corresponding plots are shown in Fig. 8(d). TTS in this case is further improved to 45.4% less than in the no-control case. Control reaction is even faster than in the P-VSL case and smoother. Capacity flow and critical occupancy are maintained most of the time as well, and in this scenario there is no peak in occupancy or reduction in flow around the start of actuation, unlike Scenarios 2 and 3.

C. Effect of the Length of the Application and Acceleration Areas

To evaluate the effect of the length of the acceleration and application areas, several scenarios with P-VSL are simulated for both areas varying one length while the other is kept fixed, using the parameters of Scenario 3 as a base. Fig. 9 summarizes the TTS results.

The conducted simulations indicate that shorter application areas improve performance. The best results were observed with application areas as short as 100 m, although results considering a 50 m long application area were very similar. Such short areas are insufficient for vehicles travelling at the nominal speed limit (100 km/h) to decelerate to the lowest possible speed limit (10 km/h) in the performed experiments. However, it should be noted that 50 and 100 m long application areas are sufficient for lesser speed variations, such as a 20 km/h change. In a typical simulation most variations of speed limit between two control periods are inside this limit.

Although simulation results show a better performance with short application areas, in the event of field application it must be taken into account that having two (or more) conflicting speed limit signs very close to each other might be confusing to drivers.

With respect to acceleration areas, best results were obtained with a length of around 175 m. Longer areas increase delay, while shorter ones are not sufficient for vehicles to accelerate to v_{cr} . Indeed, with a short acceleration area (less than 175 m) vehicles are unable to reach the critical speed at the bottleneck when very low speed limits are applied. Specifically, for the scenario referring to the point with the shortest acceleration area shown in Fig. 9(b), only the last three detectors placed in the merging area are used instead of all five, because vehicles approached the start of the merging area with very low speeds, leading to occupancies that are too high. A similar study for the case of merging control with traffic lights at work zones found better results for an acceleration area of 200 m for a section with 80 km/h speed limit [35].

The visible degradation for increasing length of either area is expected due to the introduced delay, which is more pronounced when increasing the length of the application area; and also due to the change of vehicle speed at the bottleneck when altering the length of the acceleration area.

Scenarios 5 and 6 are chosen as representative scenarios of length changes in application and acceleration areas for comparing with Scenario 3. Flows, occupancies, speeds, and VSL rates are shown in Fig. 8(e) and (f), respectively. In Fig. 8(e) the transitory effect ('void') is not noticeable because of the short application area. Also, the shorter delays lead to a faster traffic response and better performance, and allow a faster controller (with higher gain) to be used with stability. A 46.7% reduction in TTS is obtained, and all curves for Scenario 5 are smoother than for Scenario 3.

In Scenario 6 there is also a (less pronounced) reduction in delay, leading to a faster traffic response, although not as fast as in Scenario 5 (see Fig. 8(f)). Still, a 43.2% reduction in TTS is obtained.

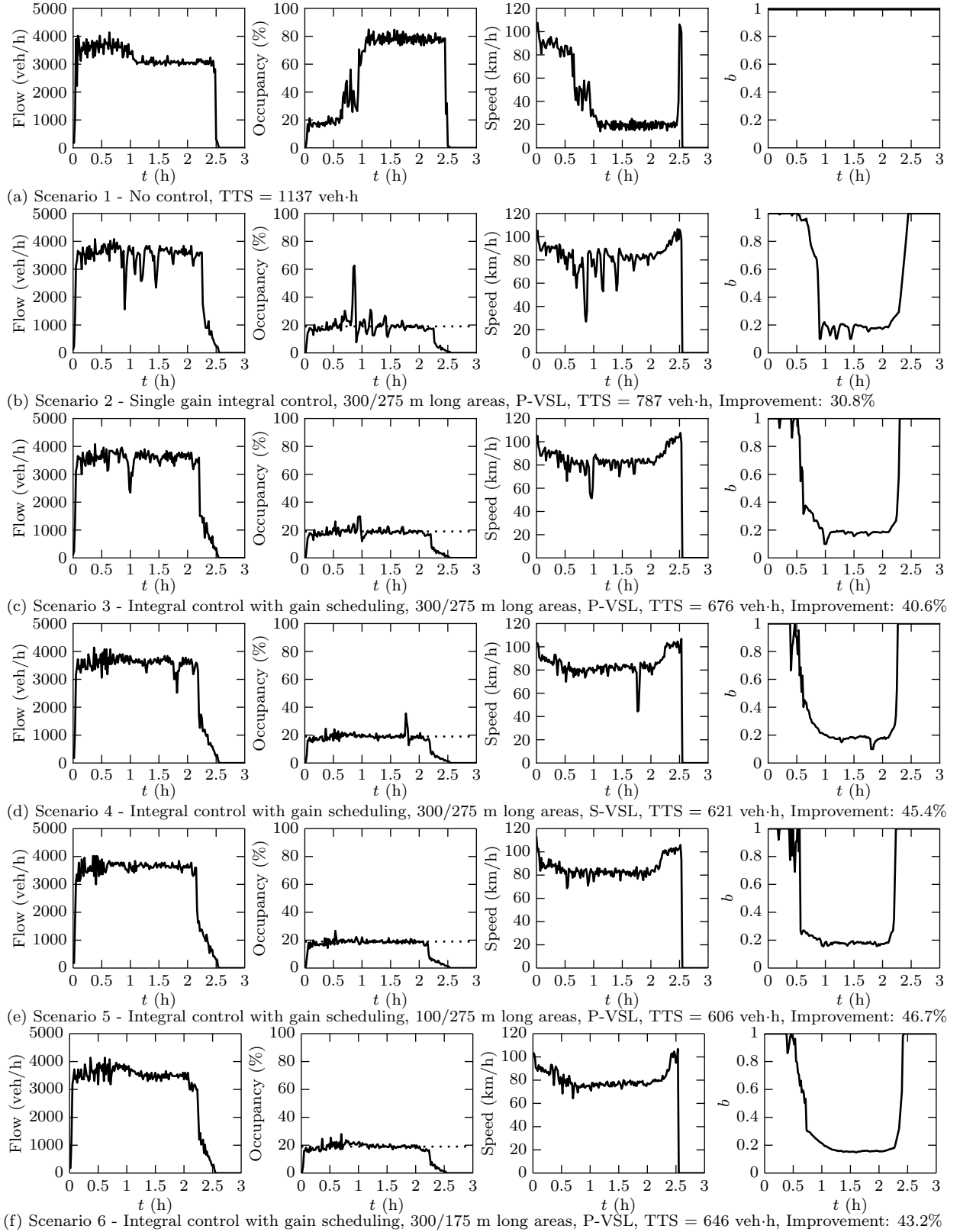


Fig. 8. Flow, occupancy and speed measured in a detector placed at the bottleneck for six different scenarios

D. Field Deployment Aspects

Table I, rows 7–9, summarizes the results for scenarios considering certain implementation aspects, keeping all other

parameters equal to those used for Scenario 3. Flows, occupancies, speeds, and VSL rates are shown in Fig. 10(a–c). For each scenario, two speeds are shown. Gray lines in the speed

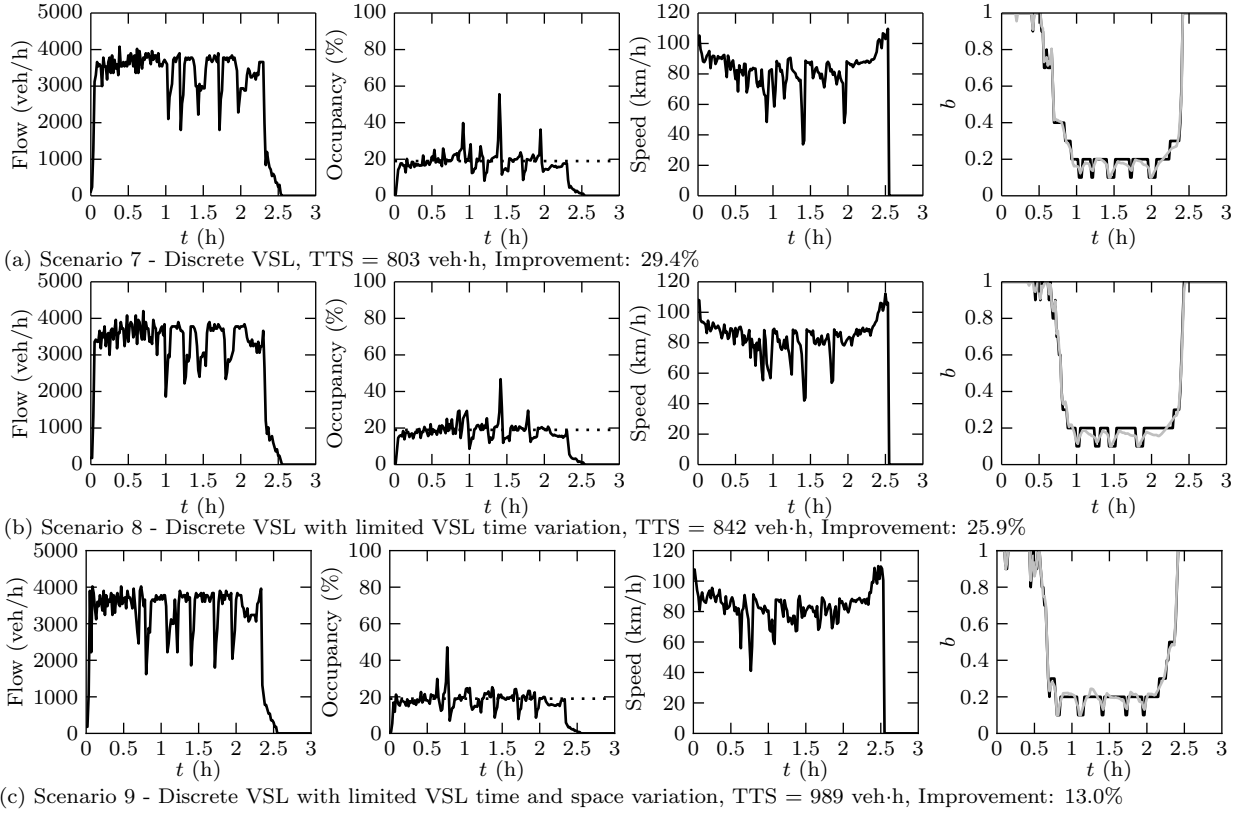


Fig. 10. Flow, occupancy and speed measured in a detector placed at the bottleneck for three different scenarios. All scenarios have gain scheduling, 300/275 m long areas and P-VSL

charts correspond to values computed by the control algorithm, while black lines correspond to the (rounded) values displayed for drivers.

1) *Discrete VSL*: for Scenario 7, only values that are multiple of 10 km/h are allowed as admissible speed limits

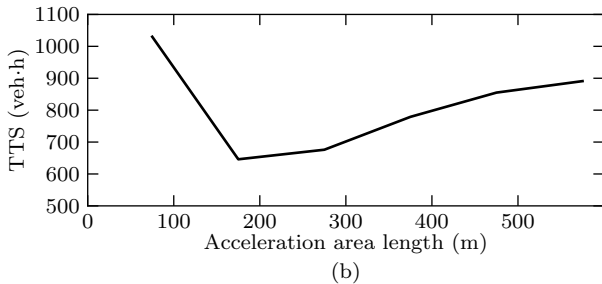
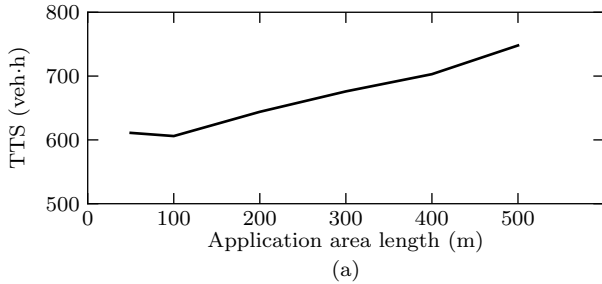


Fig. 9. Variation of TTS with the length of the (a) application and (b) acceleration areas with P-VSL and integral control with gain scheduling.

(i.e., $VSL \in \{10, 20, \dots, 90, 100\}$ km/h). Limiting controller action this way leads to a deterioration in performance. TTS is 29.4% better than in the no control case and 10% worse than in Scenario 3.

It can be seen in Fig. 10(a) that there are large variations in flow, speed and occupancy. These are caused by the controller constantly switching between 10 and 20 km/h, as it cannot assume an intermediate value and must alternate between one that is too high, and one that is too low. Since the induced flows by 10 and 20 km/h are very different, large fluctuations are inevitable.

The degradation in performance with Discrete VSL should be lower if more intermediate values were to be admissible for VSL, or if the flows induced by different speed limits approached a more linear relation, like the one modelled with the METANET simulator (Fig. 2). The first aspect is a matter of choice for the designer and authorities, while the second depends solely on the capacity flow/speed limit relation.

2) *Limited VSL time and space variation*: in Scenario 8, besides discrete VSL, we also consider that the difference between the displayed speed limit in two consecutive control intervals cannot exceed 20 km/h. Overall, results are similar to those obtained for Scenario 7, as can be seen in Fig. 10(b). There is a decrease in TTS of 25.9% in relation to the no control case, which is worse than in the previous case.

Finally, in Scenario 9 we also address VSL space variation, by considering that there are five adjacent application areas. The last one is exactly like the application area in all

other scenarios, with a length of 300 m and ending in the acceleration area. The other four application areas are located upstream, each being 500 m long. The speed limit in each of the four upstream areas is (i) never lower than that of the next downstream area; (ii) not much higher than the mean speed at the respective application area; and (iii) unless one of the first two rules applies, either 20 km/h higher than that of the adjacent downstream area, or equal to the nominal speed limit (100 km/h), whichever is lower. The purpose of rule (ii) is to avoid drivers being subjected to high speed limits while in a congested area, while rules (i) and (iii) ensure a smooth increase in speed going upstream from the application area. With this setup, spatial speed limit variation between two adjacent points in the freeway is never larger than 20 km/h. The reduction in TTS is lower than in Scenario 8. Still, an improvement of 13% in TTS is obtained. In Fig. 10(c) we can see large fluctuations in speed, occupancy and flow, just as in the two previous scenarios, but more severe.

It is noteworthy that here these practical aspects have a considerably larger effect on control performance than what was observed in [12]. This larger deterioration in performance may be related to the transitory effects of a speed limit change with P-VSL. By allowing only discrete values for b , we allow only sudden changes in b , which causes larger “voids” of vehicles when decreasing speeds (in contrast to small ones when the change in b is less abrupt). Also, by having several application areas, the transitory effects repeat in each area.

E. Space-time congestion analysis

Space-time plots are interesting for visualizing how traffic conditions evolve along the entire network. Figure 11 depicts space-time plots of vehicle speeds for Scenarios 1, 3 and 9. Speeds are represented by colors, with red for 10 km/h, deep blue for 100 km/h, and shades of red, orange, yellow, green and blue for speeds in between. The x axis shows distance measured from upstream to downstream. The on-ramp is located at $x = 4000$ m and the bottleneck is located at $x = 4075$ m. In Scenarios 3 and 9, the (last) application area starts at $x = 3500$ m and ends at $x = 3800$ m, where the acceleration area begins.

Figure 11(a) depicts vehicle speeds for the no control case. The orange region corresponds to a congested area, where vehicles travel with lower speeds. Congestion starts at around $t = 0.7$ h in the bottleneck area and grows towards upstream. After demand decreases the congestion recedes, and is finally dissolved approximately at $t = 2.5$ h.

Figure 11(b) shows vehicle speeds for Scenario 3. Here there is also a visible region with lower speeds, corresponding to the controlled congestion caused by MTFC-VSL. This region is smaller than the one in Fig. 11(a) and has a lighter color. This congestion visibly has a higher speed and lasts for less time than the congestion in the no control case. Also, in this case congestion starts at the application area instead of at the bottleneck.

Vehicle speeds for Scenario 9 can be seen in Fig. 11(c). The congested region has a pattern of yellow and orange stripes, caused by the shockwaves propagating upstream created by the

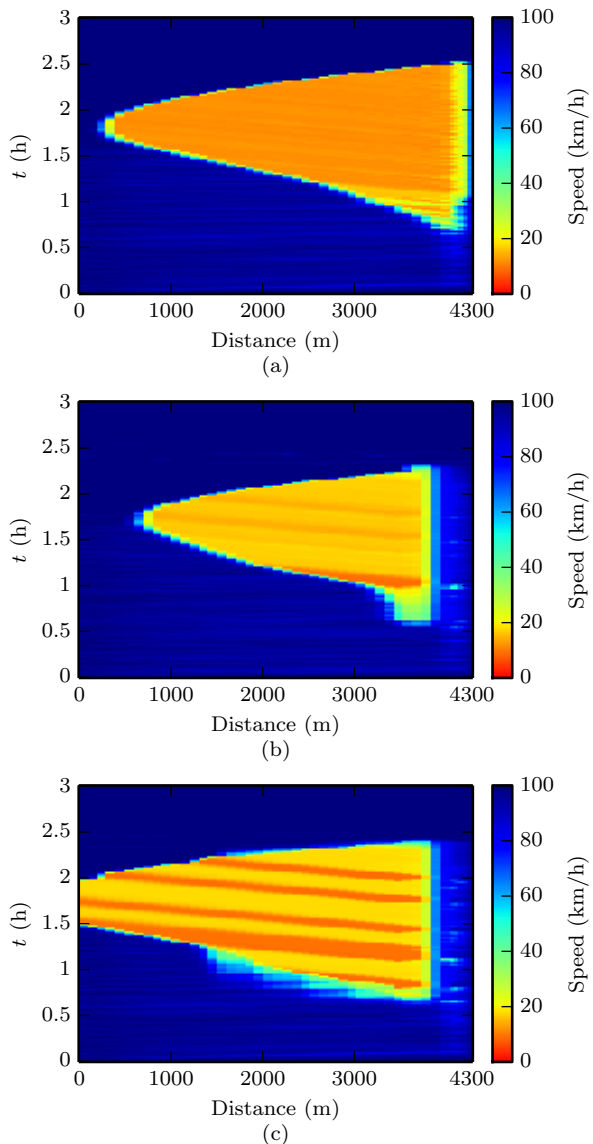


Fig. 11. Space-time diagram showing vehicle speed in the network for (a) Scenario 1, (b) Scenario 3, and (c) Scenario 9

switching of VSL between 10 and 20 km/h. The congestion duration for this scenario is between those of scenarios 1 and 3, and it stretches in space farther than any of them. However, it has (overall) a lighter color than in the no control case, indicating higher (mean) speeds (i.e., a less intense congestion) resulting in less overall time for the dissolution of congestion.

V. CONCLUSIONS

Mainstream Traffic Flow Control (MTFC) is applied upstream from an on-ramp merge bottleneck in a microscopic simulation environment by the use of Variable Speed Limits (VSL). Several control aspects not addressed in previous works based on macroscopic simulation are observed. Applying VSL in a specific location (P-VSL) rather than along an entire section (S-VSL) makes the system considerably slower and introduces transitory effects, which makes S-VSL desirable if possible. Simulation results show that shorter application

and acceleration areas decrease delay. Even with a highly nonlinear relation and P-VSL, improvements in the order of 40% in total time spent by traffic were achieved. These were obtained for a capacity drop of around 17%, so in scenarios with lower drops the benefits will not be so pronounced. The consideration of practical aspects, such as discrete VSL, show that significant improvement may be obtained in practice although their negative impact in performance seems more pronounced than previously reported. The capacity flow/speed limit relation is a vital part of the MTFC concept and should be further investigated. As is, large reductions in speed limit are necessary to induce the intended flows to avoid congestion and may affect acceptance of the method.

REFERENCES

- [1] M. Papageorgiou and A. Kotsialos, "Freeway ramp metering: an overview," *IEEE Trans. on Intel. Transp. Syst.*, vol. 3, no. 4, pp. 271–281, 2002.
- [2] M. Papageorgiou, E. Kosmatopoulos, and I. Papamichail, "Effects of variable speed limits on motorway traffic flow," *Transp. Res. Record: J. of the Transp. Res. Board*, vol. 2047, pp. 37–48, 2008.
- [3] B. Heydecker and J. Addison, "Analysis and modelling of traffic flow under variable speed limits," *Transportation Research Part C: Emerging Technologies*, vol. 19, no. 2, pp. 206–217, Apr. 2011.
- [4] A. Duret, S. Ahn, and C. Buisson, "Lane flow distribution on a three-lane freeway: General features and the effects of traffic controls," *Transportation Research Part C: Emerging Technologies*, vol. 24, pp. 157–167, Oct. 2012.
- [5] A. Hegyi, S. Hoogendoorn, M. Schreuder, H. Stoelhorst, and F. Viti, "SPECIALIST: a dynamic speed limit control algorithm based on shock wave theory," in *2008 11th International IEEE Conference on Intelligent Transportation Systems*, Beijing, China, Oct. 2008, pp. 827–832.
- [6] J. Zhang, H. Chang, and P. Ioannou, "A simple roadway control system for freeway traffic," in *2006 American Control Conference*, Minneapolis, MN, USA, 2006, pp. 4900–4905.
- [7] A. Alessandri, A. Di Febbraro, A. Ferrara, and E. Punta, "Optimal control of freeways via speed signalling and ramp metering," *Control Engineering Practice*, vol. 6, no. 6, pp. 771–780, Jun. 1998.
- [8] M. Burger, M. van den Berg, A. Hegyi, B. De Schutter, and J. Hellendoorn, "Considerations for model-based traffic control," *Transportation Research Part C: Emerging Technologies*, vol. 35, pp. 1–19, Oct. 2013.
- [9] A. Hegyi and S. P. Hoogendoorn, "Dynamic speed limit control to resolve shock waves on freeways - field test results of the SPECIALIST algorithm," in *13th International IEEE Conference on Intelligent Transportation Systems*, Funchal, Madeira Island, Portugal, Sep. 2010, pp. 519–524.
- [10] R. C. Carlson, I. Papamichail, M. Papageorgiou, and A. Messmer, "Optimal motorway traffic flow control involving variable speed limits and ramp metering," *Transp. Sc.*, vol. 44, no. 2, pp. 238–253, 2010.
- [11] —, "Optimal mainstream traffic flow control of large-scale motorway networks," *Transp. Res. Part C: Emerging Technologies*, vol. 18, no. 2, pp. 193–212, 2010.
- [12] R. C. Carlson, I. Papamichail, and M. Papageorgiou, "Local feedback-based mainstream traffic flow control on motorways using variable speed limits," *IEEE Trans. on Intel. Transp. Syst.*, vol. 12, no. 4, pp. 1261–1276, 2011.
- [13] —, "Comparison of local feedback controllers for the mainstream traffic flow on freeways using variable speed limits," *J. of Intel. Transp. Syst.: tech., plan., and oper.*, vol. 17, no. 4, pp. 268–281, 2013.
- [14] A. Messmer and M. Papageorgiou, "METANET: A macroscopic simulation program for motorway networks," *Traffic Engineering & Control*, vol. 31, no. 8-9, pp. 466–470, 1990.
- [15] P. Hidas, "Lane changing and merging under congested conditions in traffic simulations models," in *Urban Transp. XI: Urban Transp. and the Env. in the 21st Century*, Algarve, Portugal, 2005, pp. 779–788.
- [16] E. Chevallier and L. Leclercq, "Do microscopic merging models reproduce the observed priority sharing ratio in congestion?" *Transp. Res. Part C: Emerging Technologies*, vol. 17, no. 3, pp. 328–336, 2009.
- [17] K. Chung, J. Rudjanakanoknad, and M. Cassidy, "Relation between traffic density and capacity drop at three freeway bottlenecks," *Transp. Res. Part B: Methodological*, vol. 41, no. 1, pp. 82–95, 2007.
- [18] Transport Simulation Systems, "AIMSUN dynamic simulator users manual v. 7," 2012.
- [19] P. Gipps, "A behavioural car-following model for computer simulation," *Transp. Res. Part B: Methodological*, vol. 15, no. 2, pp. 105–111, 1981.
- [20] —, "A model for the structure of lane-changing decisions," *Transp. Res. Part B: Methodological*, vol. 20, no. 5, pp. 403–414, 1986.
- [21] H. Chang, Y. Wang, J. Zhang, and P. Ioannou, "An integrated roadway controller and its evaluation by microscopic simulator VISSIM," in *European Control Conference 2007*, Kos, Greece, 2007, pp. 2436–2441.
- [22] A. Hegyi, M. Burger, B. De Schutter, J. Hellendoorn, and T. J. J. van den Boom, "Towards a practical application of model predictive control to suppress shock waves on freeways," in *European Control Conference 2007*, Kos, Greece, 2007, pp. 1764–1771.
- [23] B. G. Ros, V. L. Knoop, B. van Arem, and S. P. Hoogendoorn, "Mainstream traffic flow control at sags," in *The Transportation Research Board (TRB) 93rd Annual Meeting*, Washington, D.C., USA, 2014.
- [24] X. Y. Lu and S. E. Shladover, "Review of variable speed limits and advisories: theory, algorithms and practice," *Transp. Res. Record: J. of the Transp. Res. Board*, vol. 2423, pp. 15–23, 2014.
- [25] R. C. Carlson, "Mainstream traffic flow control on motorways," Doctor of Philosophy, Technical University of Crete, Chania, Greece, 2011. [Online]. Available: <http://www.library.tuc.gr/artemis/PD2012-0015/PD2012-0015.pdf>
- [26] G. Iordanidou, C. Roncoli, I. Papamichail, and M. Papageorgiou, "Feedback-based mainstream traffic flow control for multiple bottlenecks on motorways," *IEEE Trans. on Intel. Transp. Syst.*, Early Access.
- [27] M. S. Fadali and A. Visioli, *Digital Control Engineering: Analysis and Design*, 2nd ed. Boston: Academic Press, 2013.
- [28] K. Gao, "Multi-objective traffic management for livability," M.S. thesis, TU Delft, Delft, The Netherlands, 2012.
- [29] Å. Björck, *Numerical methods for least squares problems*. SIAM, 1996.
- [30] A. Hegyi, *Model predictive control for integrating traffic control measures*. Delft, The Netherlands: TRAIL Research School, Delft University of Technology, 2004.
- [31] K. J. Astrom and B. Wittenmark, *Adaptive Control*, 2nd ed. Addison-Wesley, 1995.
- [32] W. J. Schakel and B. van Arem, "Improving traffic flow efficiency by in-car advice on lane, speed, and headway," *IEEE Transactions on Intelligent Transportation Systems*, pp. 1–10, 2014. [Online]. Available: <http://ieeexplore.ieee.org/lpdocs/epic03/wrapper.htm?arnumber=6747406>
- [33] Y. Wang and P. A. Ioannou, "New model for variable speed limits," *Transp. Res. Record: J. of the Transp. Res. Board*, vol. 2249, pp. 38–43, 2011.
- [34] E. R. Müller, R. C. Carlson, W. Kraus Jr., and M. Papageorgiou, "Microscopic simulation analysis of mainstream traffic flow control with variable speed limits," in *16th International IEEE Conference on Intelligent Transport Systems*, The Hague, The Netherlands, 2013.
- [35] A. Tympakianaki, A. Spiliopoulou, A. Kouvelas, I. Papamichail, M. Papageorgiou, and Y. Wang, "Real-time merging traffic control for throughput maximization at motorway work zones," *Transportation Research Part C: Emerging Technologies*, vol. 44, pp. 242–252, Jul. 2014.



Eduardo Rauh Müller was born in Florianópolis, Brazil, in 1988. He received the Bel.Eng. degree in control and automation engineering and the Me.Eng. degree in automation and systems engineering from the Federal University of Santa Catarina, Florianópolis, Brazil, in 2011 and 2013, respectively. Since 2014, he is a doctorate student at the same university. His research interests include automatic control and optimization theory applied to traffic and transportation systems.



Rodrigo Castelan Carlson was born in Florianópolis, Brazil, in 1980. He received the Bel.Eng. degree in control and automation engineering and the Me.Eng. degree in electrical engineering from the Federal University of Santa Catarina, Florianópolis, Brazil, in 2004 and 2006, respectively, the Bachelor's degree in business administration from the University of the State of Santa Catarina, Florianópolis, Brazil, in 2006, and the Ph.D. degree in Production Engineering and Management from the Technical University of Crete, Chania, Greece, in 2011.

From 2006 to 2007, he was a Research and Development Engineer with Department of Automation and Systems, Federal University of Santa Catarina. From 2007 to 2011, he was a Research Assistant with the Dynamic Systems and Simulation Laboratory, Technical University of Crete. From 2011 to 2012 he was a post-doctoral researcher with the Department of Automation and Systems, Federal University of Santa Catarina. Since 2012 he is an Assistant Professor with the Center for Mobility Engineering, Federal University of Santa Catarina, Joinville, Brazil. He is the author and co-author of several technical papers in scientific journals and magazines and in scientific conference proceedings. His research interests include automatic control and optimization theory and applications to traffic and transportation systems.

Dr. Carlson was the recipient of a scholarship for postgraduate studies abroad from The Capes Foundation, Ministry of Education of Brazil (during 2007–2011) and the Gold Medal of the Young European Arena of Research 2010 in the pillar “Mobility and Intermodality.”



Werner Kraus Jr. was born in Blumenau, Brazil, in 1964. He holds B.El. Eng. (1986) and M.El.Eng. (1991) degrees from the Federal University of Santa Catarina, Brazil, and a Ph.D. (1997) from the Australian National University. Since 2000 he has been with the Department of Automation and Systems Engineering at the Federal University of Santa Catarina. His main interests are control of urban mobility systems and cooperative systems for traffic management and control, with emphasis in the implementation of prototype systems in real scenarios.



Markos Papageorgiou received the Diplom-Ingenieur and Doktor-Ingenieur (honors) degrees in Electrical Engineering from the Technical University of Munich, Germany, in 1976 and 1981, respectively. He was a Free Associate with Dorsch Consult, Munich (1982-1988), and with Institute National de Recherche sur les Transports et leur Sécurité (INRETS), Arcueil, France (1986-1988). From 1988 to 1994 he was a Professor of Automation at the Technical University of Munich. Since 1994 he has been a Professor at the Technical University of Crete,

Chania, Greece. He was a Visiting Professor at the Politecnico di Milano, Italy (1982), at the Ecole Nationale des Ponts et Chaussées, Paris (1985-1987), and at MIT, Cambridge (1997, 2000); and a Visiting Scholar at the University of California, Berkeley (1993, 1997, 2001, 2011) and other universities.

Dr. Papageorgiou is author or editor of 5 books and of over 400 technical papers. His research interests include automatic control and optimization theory and applications to traffic and transportation systems, water systems and further areas. He was the Editor-in-Chief of *Transportation Research – Part C* (2005-2012). He also served as an Associate Editor of IEEE Control Systems Society – Conference Editorial Board, of *IEEE Transactions on Intelligent Transportation Systems* and other journals. He is a Fellow of IEEE (1999) and a Fellow of IFAC (2013). He received a DAAD scholarship (1971-1976), the 1983 Eugen-Hartmann award from the Union of German Engineers (VDI), and a Fulbright Lecturing/Research Award (1997). He was a recipient of the IEEE Intelligent Transportation Systems Society *Outstanding Research Award* (2007) and of the IEEE Control Systems Society *Transition to Practice Award* (2010). He was presented the title of Visiting Professor by the University of Belgrade, Serbia (2010). The Dynamic Systems and Simulation Laboratory he has been heading since 1994, received the IEEE Intelligent Transportation Systems Society *ITS Institutional Lead Award* (2011). He was awarded an ERC Advanced Investigator Grant (2013-2017).